MATERIALS SCIENCE / МАТЕРИАЛОВЕДЕНИЕ

UDC 669:539.381.296
DOI 10.17073/0368-0797-2024-6-679-685

Original article
Оригинальная статья

INHOMOGENEITY OF DEFORMATION OF SURFACED STAINLESS STEEL

S. P. Buyakova[1], K. N. Kayurov[2], S. A. Barannikova[1]

[1] **Institute of Strength Physics and Materials Science, Siberian Branch of the Russian Academy of Sciences** (2/4 Akademicheskii Ave., Tomsk 634055, Russian Federation)
[2] **LLK Scientific Production Enterprise of Geophysical Equipment "Luch"** (34 2nd Yurginskaya Str., Novosibirsk 630051, Russian Federation)

bsa@ispms.ru

Abstract. The work is devoted to the study of the inhomogeneity of deformation of steel samples with laser surfacing. Highly nitrogenous austenitic stainless steel of the 08Kh18N6AG10S grade was selected as the substrate material in the state as received. To improve the mechanical properties of structural elements that operate under conditions of impact and abrasive wear, a surfacing of Ni–7Cr–6Fe + 60 % WC composite powder was applied to the steel. The surfacing was carried out with a change in the power of laser radiation from 1 to 3 kW and a change in the scanning speed from 0.005 to 0.040 m/s. The penetration depth of a single roller decreases with increasing the scanning speed. The microhardness varies widely in the surfacing thickness (from 7,000 ± 80 to 13,500 ± 70 MPa) and decreases with increasing scanning speed. Using the speckle photography method in the process of uniaxial extension of flat samples, it was found that the modes of laser surfacing also affect the level of inhomogeneity of deformation of micro-volumes of the deposited layer and the substrate. At the elastoplastic transition, the coefficient of variation of local deformations in the sample increases with an increase in the specific energy of laser surfacing. Coatings made of Ni–Cr–Fe+WC composite powder, obtained by laser surfacing under specified conditions, make it possible to increase the hardness and service life of structural elements of rotary controlled systems made of 08Kh18N6AG10S steel.

Keywords: plastic deformation, localization, surfacing, stainless steel, mechanical properties

Acknowledgements: The work was performed within the framework of the complex project "Organization of high-tech production of rotary controlled systems for opening complex plates and drilling wells with a large deviation from the vertical in difficult geological conditions in the Arctic" (grant agreement No. 075-11-2022-019 dated April 06, 2022), implemented by the Institute of Strength Physics and Materials Science of the Siberian Branch of the Russian Academy of Sciences with the financial support of the Ministry of Education and Science of the Russian Federation in the framework of Government Decree No. 218 dated 04.09.2010.

For citation: Buyakova S.P., Kayurov K.N., Barannikova S.A. Inhomogeneity of deformation of surfaced stainless steel. *Izvestiya. Ferrous Metallurgy*. 2024;67(6):679–685. https://doi.org/10.17073/0368-0797-2024-6-679-685

Исследование неоднородности деформации нержавеющей стали с наплавкой

С. П. Буякова[1], К. Н. Каюров[2], С. А. Баранникова[1]

[1] **Институт физики прочности и материаловедения Сибирского отделения РАН** (Россия, 634055, Томск, Академический пр., 2/4)
[2] **ООО Научно-производственное предприятие геофизической аппаратуры «ЛУЧ»** (Россия, 630051, Новосибирск, ул. 2-я Юргинская, 34)

bsa@ispms.ru

Аннотация. Работа посвящена изучению неоднородности деформации стальных образцов с лазерной наплавкой. В качестве материала подложки была выбрана высокоазотистая аустенитная нержавеющая сталь марки 08Х18Н6АГ10С в состоянии поставки. Для повышения механических свойств конструктивных элементов, работающих в условиях ударно-абразивного изнашивания, на сталь наносили наплавку из композиционного порошка Ni–7Cr–6Fe + 60 % WC. Наплавку проводили при изменении мощности лазерного излучения (1 – 3 кВт) и скорости сканирования (0,005 – 0,040 м/с). Глубина проплавления одиночного валика уменьшается с увеличением скорости сканирования. Микротвердость варьируется в широких пределах по толщине наплавки (с 7000 ± 80 до 13 500 ± 70 МПа) и уменьшается с увеличением скорости сканирования. С использованием метода спекл-фотографии в процессе одноосного растяжения плоских образцов установлено, что режимы лазерной наплавки также влияют на уровень неоднородности деформации микрообъемов наплавленного слоя и подложки. На упругопластическом переходе коэффициент вариации локальных деформаций в образце увеличивается

с ростом удельной энергии лазерной наплавки. Покрытия из композиционного порошка Ni–Cr–Fe+WC, полученные методом лазерной наплавки при заданных режимах, позволяют повысить твердость и ресурс конструктивных элементов роторных управляемых систем, изготовленных из стали марки 08Х18Н6АГ10С.

Ключевые слова: пластическая деформация, локализация, наплавка, нержавеющая сталь, механические свойства

Благодарности: Работа выполнена в рамках комплексного проекта «Организация высокотехнологичного производства роторных управляемых систем для вскрытия сложных пластов и бурения скважин с большим отходом от вертикали в сложных геологических условиях, Арктике» (соглашение о предоставлении субсидии от 06 апреля 2022 № 075-11-2022-019), реализуемого Институтом физики прочности и материаловедения Сибирского отделения РАН при финансовой поддержке Минобрнауки России в рамках постановления Правительства РФ от 09.04.2010 № 218.

Для цитирования: Буякова С.П., Каюров К.Н., Баранникова С.А. Исследование неоднородности деформации нержавеющей стали с наплавкой. *Известия вузов. Черная металлургия*. 2024;67(6):679–685. https://doi.org/10.17073/0368-0797-2024-6-679-685

Introduction

The increasing volume of hydrocarbon recovery requires complex well design profiles, where trajectories often include curved and inclined-rectilinear sections of significant length. For drilling such wells, rotary controlled systems (RCS) are employed as drill bit drives [1; 2]. The components of these systems are made from non-magnetic austenitic stainless steels [3; 4]. Under high loads, these elements develop defects that may lead to failures, with incidents most frequently occurring during rotary drilling operations in wells.

The hardness and wear resistance of steel surfaces can be enhanced by applying metal-ceramic (MC) coatings [5 – 7]. These coatings, a type of metal-matrix composite, consist of a metallic matrix reinforced with ceramic particles. Ceramic phases provide high hardness, while the relatively soft matrix holds the ceramic particles, imparting high fracture resistance and strength to the composite [8 – 11]. Metal-ceramic materials are highly resistant to abrasive wear.

One of the most widely used reinforcing materials for creating MC coatings is tungsten carbide (WC), known for its high hardness and strength [12 – 16]. These properties make WC-based coatings widely used for strengthening the working surfaces of wear-prone machine parts and mining tools. However, surfacing austenitic steels is challenging due to their tendency to form hot cracks during crystallization [17]. Solidification cracks in weld metal are considered the most detrimental and are more frequently observed than other types of cracking. The structure of austenitic steels is highly dependent on their chemical composition and the thermophysical conditions of crystallization, which are determined by the processing method [8; 17].

Technologies for additive manufacturing through layer-by-layer surfacing are rapidly developing [18 – 20]. These technologies enable the production of components with diverse geometric shapes, including large-scale parts, while also reducing material consumption. Such methods yield products with mechanical properties superior to those achieved through traditional manufacturing techniques. Layer-by-layer surfacing can be accomplished using various methods, with heat sources such as lasers, electron beams, electric arcs, and plasma arcs. Regardless of the method and type of material used, one of the critical features of additive manufacturing through layer-by-layer surfacing is the anisotropy of mechanical properties. This anisotropy arises from the crystallization process of the metal, leading to heterogeneous structures within the deposited layer and transcrystalline grain growth. Technologies utilizing concentrated energy sources offer significant potential for addressing these challenges.

Given that processes occurring near the interface during laser surfacing can impact the material's mechanical properties, this study aimed to investigate the effect of laser surfacing parameters on the inhomogeneity of plastic deformation in austenitic steel with surfacing.

Materials and methods

Forgings made of non-magnetic, high-nitrogen chromium-nickel-manganese stainless steel of the 08Kh18N6AG10S grade were used as the substrate material. The chemical composition of the steel was as follows, wt. %: <0.06 C; 16.0 – 18.0 Cr; 5.0 – 6.0 Ni; >0.4 N; 8.5 – 10.0 Mn; 0.6 – 1.2 Si; balance Fe. Currently, 08Kh18N6AG10S steel has demonstrated positive application experience in geophysical instruments, showing higher ductility and impact toughness compared to imported analogs while maintaining increased strength properties [21]. The austenitic stainless steel of the 08Kh18N6AG10S grade, in the as-received state, has an average yield strength of 800 MPa, an ultimate tensile strength of 1000 MPa, and an elongation at break of up to 20 %. The microstructure and phase composition of the steel have been described in detail in [21].

Laser surfacing of the Fe–Cr–Mn–Ni–N steel plates was performed using Ni–7Cr–6Fe + 60 % WC powder on an experimental setup at the Institute of Strength Physics and Materials Science of the Siberian Branch of the Russian Academy of Sciences (ISPMS SB RAS). The surfacing material was a nickel-based alloy with

a high content of tungsten carbide particles uniformly distributed within the solid matrix, which had a hardness exceeding 63 HRC. The particle size of tungsten carbide ranged from 10 to 45 μm, ensuring maximum resistance to abrasive and erosive wear. Surfacing parameters were selected to achieve a uniform, monolithic coating based on pre-established technological conditions. The beam diameter (d) was 4 mm, the power of the LS-15 fiber laser ranged from 1 to 3 kW, the scanning speed (V) ranged from 0.005 to 0.040 m/s, and the powder feed rate (F) was 20 mg/s.

Flat samples with dimensions of 50×8×2 mm in the working section were cut from the billets using the electro-spark method. The thickness of the Ni–7Cr–6Fe + 60 % WC surfacing layer was 1 mm, and the substrate layer (Fe–Cr–Mn–Ni–N) was 7 mm. The prepared samples were subjected to uniaxial tensile testing at room temperature on a Walter + Bai AG universal testing machine (LFM 125 series). The displacement rate of the movable grip V_{mach} was 0.4 mm/min, corresponding to a deformation rate of $1.67 \cdot 10^{-4}$ s^{-1}.

Structural studies were conducted using light microscopy (AXIOVERT-200MAT microscope) and X-ray diffraction analysis (DRON-07 diffractometer). The distribution of chemical elements across the thickness of the base and surfacing metal was measured using a LEO EVO 50 scanning electron microscope (Carl Zeiss, Germany) equipped with an Oxford Instruments attachment for X-ray dispersive microanalysis (Nanotech Center of ISPMS SB RAS). Microhardness measurements were performed using an instrumented indentation method in accordance with GOST R 8.748–2011 (ISO 14577-1:2002) on a PMT-3 microhardness tester.

Deformation fields on the surface of flat samples were recorded during mechanical testing using the speckle photography method outlined in [22–25]. The local elongation along the tensile axis of the sample, denoted as ε_{xx}, is typically the most intuitive parameter for visualizing and analyzing components of the plastic distortion tensor. To quantitatively evaluate the deformation inhomogeneity of the substrate and surfacing, the coefficient of variation was determined as the ratio of the standard deviation to the mean value [26].

Research results

During laser surfacing, powder granules melt, and the liquid alloy wets the tungsten carbide particles. As a result of subsequent high-speed crystallization, a metal-ceramic coating is formed. Mechanical testing revealed that surface hardening of the austenitic steel increased its tensile strength to 1500 MPa while reducing its ductility by 6 %.

To achieve metallurgical bonding between the surfacing material and the steel substrate while preventing dilution of the coating by the substrate material, surfacing must be performed under optimal conditions. Preventing crack formation requires applying different surfacing modes when depositing a single roller. The geometric parameters of the surfacing beads (coating thickness, penetration depth into the steel, and bead width) depend on the scanning speed, powder feed rate, and laser power. To optimize surfacing conditions, with constant powder feed rate and laser beam diameter, the scanning speed V and laser power P were chosen as variable factors (see Table). These parameters allow adjusting the specific energy, calculated as described in [17]:

$$E = \frac{P}{Vd},$$

where E is the specific energy, P is the laser power, d is the beam diameter, and V is the scanning speed.

Fig. 1 illustrates the effect of specific energy (E) on the penetration depth (L) of 08Kh18N6AG10S steel. The reduction in penetration depth with increasing scanning speed is attributed to the lower energy absorption during laser surfacing. As scanning speed increases, the proportion of the surface area covered by tungsten carbide (WC) particles grows, thereby reducing the mixing zone depth between the Ni–7Cr–6Fe + 60 % WC powder and the steel substrate.

X-ray diffraction analysis and dispersive microanalysis revealed that the content of the main alloying elements in the base metal corresponds to the nominal composition of 08Kh18N6AG10S steel. During heating, diffusion of alloying elements occurs from the base metal into the surfacing layer, while carbon diffuses in the opposite direction. At the interface on the austenitic steel side, reduced concentrations of manganese, chromium, and nitrogen were observed, along with an increased concentration of iron. No visible inclusions of ferrite or σ-phase were detected in the base metal (08Kh18N6AG10S) or the heat-affected

Effect of laser surfacing modes on the composite phase composition

Влияние режимов лазерной наплавки на фазовый состав композита

No.	P, kW	V, m/s	Phase
1	1.50	0.012	γ-Fe, $Me_{23}C_6$, WC, W_2C
2	1.50	0.016	γ-Fe, $Me_{23}C_6$, WC, W_2C
3	1.75	0.016	γ-Fe, $Me_{23}C_6$, WC, W_2C
4	2.00	0.020	γ-Fe, $Me_{23}C_6$, WC, W_2C
5	2.00	0.030	γ-Fe, $Me_{23}C_6$, WC, W_2C
6	2.00	0.035	γ-Fe, $Me_{23}C_6$, WC, W_2C
7	1.50	0.008	γ-Fe, $Me_{23}C_6$, WC, W_2C, Me_6C
8	2.00	0.008	γ-Fe, $Me_{23}C_6$, WC, W_2C, Me_6C

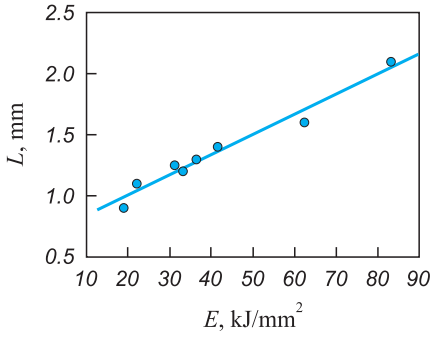

Fig. 1. Effect of specific energy (scanning speed and laser power) on the penetration depth of 08Kh18N6AG10S steel

Рис. 1. Влияние удельной энергии (скорости сканирования и мощности лазера) на глубину проплавления стали марки 08Х18Н6АГ10С

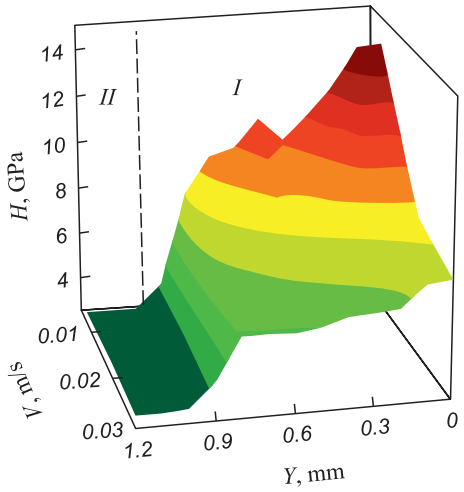

Fig. 2. Effect of scanning speed on microhardness distribution in the sample at a laser power of 2 kW (dashed line – connection zone):
I – Ni–Cr–Fe + WC surfacing layer; *II* – 08Kh18N6AG10S steel

Рис. 2. Влияние скорости сканирования на распределение микротвердости в образце при мощности лазера 2 кВт (зона соединения показана штриховой линией):
I – слой наплавки Ni–Cr–Fe + WC; *II* – сталь 08Х18Н6АГ10С

zone (HAZ). In the HAZ, a distinct dendrite junction line was observed. Microstructural analysis of the laser surfacing layer identified several zones: a columnar structure oriented normal to the interface with the substrate and a mixed structure comprising fine equiaxed dendrites and lamellar eutectic formations located at grain boundaries. The microstructure consists of various carbides, including undissolved (WC), partially dissolved (W_2C), and precipitated carbides ($Me_{23}C_6$ and Me_6C) within an austenitic matrix (refer to the Table, where *Me* = Cr, Fe, W, and Ni). The volume fraction of these precipitates varies depending on the surfacing parameters, directly influencing changes in microhardness.

Measurements indicated that the average microhardness of the base metal is 3285 ± 80 MPa, while in the connection zone with the surfacing layer, it reaches 3995 ± 70 MPa (Fig. 2). The microhardness of the surfacing layer, composed of Ni–Cr–Fe + WC, varies from 7000 ± 80 to 13,500 ± 70 MPa, depending on the surfacing modes (Fig. 2). The maximum microhardness is achieved at a low scanning speed during laser surfacing. This can be attributed to the high mass fraction of WC particles at lower scanning speeds and the enhanced dissolution of WC within the matrix. Increasing the scanning speed reduces the volumetric fraction of carbides, thereby decreasing the microhardness of the surfacing layer. Additionally, at low scanning speeds, a gradual decrease in microhardness is observed with increasing depth from the surface. This is explained by variations in the content and morphology of WC particles. Such a graded microstructure can be beneficial for maximizing wear resistance without compromising the strength of the surfacing layer. Conversely, higher scanning speeds result in a more uniform distribution of microhardness throughout the depth. These variations in microhardness are linked to the formation of composite microstructures consisting of various carbides dispersed within the stainless steel matrix.

Speckle photography data on local deformations ε_{xx} revealed areas of localized deformation in both the base metal and the surfacing layers (Fig. 3).

The analysis shows that plastic deformation is concentrated in specific zones of the sample, while other regions of the material remain nearly undeformed under the same increase in deformation. To quantitatively evaluate the degree of deformation inhomogeneity across different layers, the coefficient of variation of local deformations (ν) was used. For $\nu > 0.4$, the distribution of local elongations along the sample length $\varepsilon_{xx}(x_i)$ becomes significantly non-uniform, making the average value $\langle\varepsilon_{xx}\rangle$ unrepresentative [26].

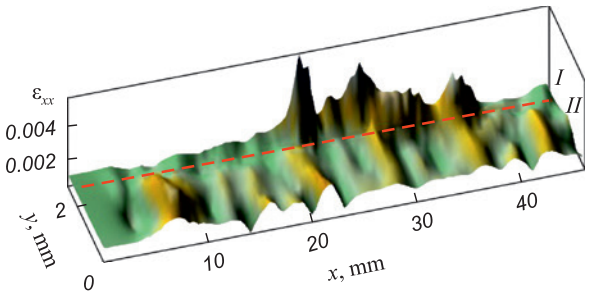

Fig. 3. Distribution of local deformations in the sample at scanning speed of 0.020 m/s and laser power of 2 kW (dashed line – connection zone):
I – Ni–Cr–Fe + WC surfacing layer; *II* – 08Kh18N6AG10S steel

Рис. 3. Распределение локальных деформаций в образце при скорости сканирования 0,020 м/с и мощности лазера 2 кВт (зона соединения показана штриховой линией):
I – слой наплавки Ni–Cr–Fe + WC; *II* – сталь 08Х18Н6АГ10С

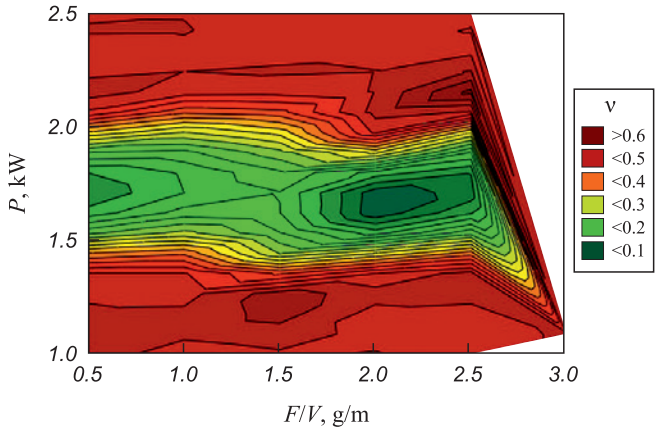

Fig. 4. Effect of laser surfacing modes on inhomogeneity degree of local deformations in the sample at total deformation of 0.01

Рис. 4. Влияние режимов лазерной наплавки на степень неоднородности локальных деформаций в образце при общей деформации 0,01

The structural inhomogeneity near the interface between the surfacing layer and the substrate significantly affects the development of localized deformation. For deformation compatibility at the composite interface, the deformations in the microvolumes adjacent to the boundary must be equal. As a result, the levels of deformation inhomogeneity in the microvolumes of different layers, measured by the coefficient of variation n, should also be balanced. Achieving this balance contributes to a more complex stress state in these regions.

Fig. 4 illustrates the variation in the deformation inhomogeneity n in a sample with surfacing under different modes during the initial stages of deformation, at a total deformation $\varepsilon = 0.01$. Upon reaching the yield strength, the levels of deformation inhomogeneity in the stainless steel and the surfacing layer differ significantly, depending on the increase in total deformation and specific energy.

A detailed analysis of microhardness distribution and deformation inhomogeneity in the composite revealed that laser surfacing modes with a laser power of 1.5 – 2.0 kW and scanning speeds of 0.007 – 0.040 m/s ensure satisfactory geometric parameters of the surfacing beads and the absence of cracks in the material.

Conclusions

To maintain the mechanical properties of the composite (steel – surfacing), it is crucial to select laser surfacing parameters that minimize deformation heterogeneity in the microvolumes of both the surfacing layer and the base metal.

The study demonstrated the effect of laser surfacing parameters on the distribution of microhardness and local deformations during the early stages of plastic deformation in 08Kh18N6AG10S stainless steel with a Ni – Cr – Fe + WC composite powder surfacing layer.

Coatings made from Ni – 7Cr – 6Fe + 60 % WC, composite powder, applied using laser surfacing at a power of 1.5 – 2.0 kW and scanning speeds of 0.007 – 0.040 m/s, are recommended to enhance the hardness and service life of structural elements in rotary controlled systems manufactured from 08Kh18N6AG10S steel.

References / Список литературы

1. Shevchenko I.A. Drilling wells with a large departure from the vertical, using a rotary-driven systems with control geophysical parameters in real-time. *Sovremennaya nauka: aktual'nye problemy teorii i praktiki. Seriya: estestvennye i tekhnicheskie nauki*. 2014;(1-2):36–39. (In Russ.).

   Шевченко И.А. Бурение скважин с большим отходом от вертикали с использованием роторных управляемых систем при контроле геофизических параметров в режиме реального времени. *Современная наука: актуальные проблемы теории и практики. Серия: естественные и технические науки*. 2014;(1-2):36–39.
2. Zakirov A.Ya. The first test results of Russian-made rotary-controlled systems. *Pro neft'. Professional'no o nefti*. 2016;(2(2)):43–47. (In Russ.).

   Закиров А.Я. Первые результаты испытаний роторно-управляемых систем российского производства. *Pro нефть. Профессионально о нефти*. 2016;(2(2)):43–47.
3. Speidel M., Speidel H. Austenitic stainless steels of high strength and ductility. *International Journal of Materials Research*. 2004;95(7):596–600. http://doi.org/10.1515/ijmr-2004-0115
4. Kostina M.V., Rigina L.G. Nitrogen-containing steels and methods of their production. *Izvestiya. Ferrous Metallurgy*. 2020;63(8):606–622. (In Russ.). https://doi.org/10.17073/0368-0797-2020-8-606-622

   Костина М.В., Ригина Л.Г. Азотосодержащие стали и способы их производства. *Известия вузов. Черная металлургия*. 2020;63(8):606–622. https://doi.org/10.17073/0368-0797-2020-8-606-622
5. Nurminen J., Näkki J., Vuoristo P. Microstructure and properties of hard and wear resistant MMC coatings deposited by laser cladding. *The International Journal of Refractory Metals and Hard Materials*. 2009;27(2):472–478. http://doi.org/10.1016/j.ijrmhm.2008.10.008
6. Zhong M., Liu W., Zhang Y., Zhu X. Formation of WC/Ni hard alloy coating by laser cladding of W/C/Ni pure element powder blend. *International Journal of Refractory Metals and Hard Materials*. 2006;24(6):453–460. http://doi.org/10.1016/j.ijrmhm.2005.09.002
7. Luo D., Hellman J., Luhulima D., Liimatainen J., Lindroos V.K. Interactions between tungsten carbide (WC) particulates and metal matrix in WC-reinforced composites. *Materials Science and Engineering: A*. 2003;340(1-2):155–162. http://doi.org/10.1016/S0921-5093(02)00173-9
8. Zhang Z., Yu T., Kovacevic R. Erosion and corrosion resistance of laser cladded AISI 420 stainless steel reinforced with VC. *Applied Surface Science*. 2017;410:225–240. http://doi.org/10.1016/j.apsusc.2017.03.137

9. Xiao Q., Sun W.-L., Yang K.-X., Xing X.-F., Chen Z.-H., Zhou H.-N., Lu J. Wear mechanisms and micro-evaluation on WC particles investigation of WC-Fe composite coatings fabricated by laser cladding. *Surface and Coatings Technology*. 2021;420:127341. http://doi.org/10.1016/j.surfcoat.2021.127341

10. Lee H.K. Effects of the cladding parameters on the deposition efficiency in pulsed Nd:YAG laser cladding. *Journal of Materials Processing Technology*. 2008;202(1-3):321–327. http://doi.org/10.1016/j.jmatprotec.2007.09.024

11. Hu G., Yang Y., Qi K., Lu X., Li J. Investigation of the microstructure and properties of NiCrBSi coating obtained by laser cladding with different process parameters. *Transactions of the Indian Institute of Metals*. 2020;73(10):2623–2634. http://doi.org/10.1007/s12666-020-02065-w

12. Huang S.W., Samandi M., Brandt M. Abrasive wear performance and microstructure of laser clad WC/Ni layers. *Wear*. 2004;256(11-12):1095–1105. https://doi.org/10.1016/S0043-1648(03)00526-X

13. Van Acker K., Vanhoyweghen D., Persoons R., Vangrunderbeek J. Influence of tungsten carbide particle size and distribution on the wear resistance of laser clad WC/Ni coatings. *Wear*. 2005;258(1-4):194–202. https://doi.org/10.1016/j.wear.2004.09.041

14. Yang J., Liu F., Miao X., Yang F. Influence of laser cladding process on the magnetic properties of WC-FeNiCr metal-matrix composite coatings. *Journal of Materials Processing Technology*. 2012;212(9):1862–1868. https://doi.org/10.1016/j.jmatprotec.2012.04.009

15. Si S.-H., Yuan X.-M., Liu Y.-L., He Y.-Z., Keesam Sh. Effect of laser power on microstructure and wear resistance of WCP/Ni cermet coating. *Journal of Iron and Steel Research International*. 2006;13:74–78. https://doi.org/10.1016/S1006-706X(06)60065-4

16. Guo Ch., Chen J., Zhou J., Zhao J., Wang L., Yu Y., Zhou H. Effects of WC–Ni content on microstructure and wear resistance of laser cladding Ni-based alloys. *Surface and Coatings Technology*. 2012;206(8-9):2064–2071. https://doi.org/10.1016/j.surfcoat.2011.06.005

17. Anandan S., Pityana L., Majumdar J.D. Structure-property-correlation in laser surface alloyed AISI 304 stainless steel with WC + Ni + NiCr. *Materials Science and Engineering: A*. 2012;536:159–169. https://doi.org/10.1016/j.msea.2011.12.095

18. Durst G. A new development in metal cladding. *JOM*. 1956; 8(3):328–333. https://doi.org/10.1007/BF03377692

19. Bogue R. Fifty years of the laser: its role in material processing. *Assembly Automation*. 2010;30(4):317–322. http://doi.org/10.1108/01445151011075771

20. Han T., Zhou K., Chen Z., Gao Y. Research progress on laser cladding alloying and composite processing of steel materials. *Metals*. 2022;12(12):2055. https://doi.org/10.3390/met12122055

21. Gordienko A.I., Abdulmenova E.V., Kozlova T.V., Gomorova Yu.F., Vlasov I.V., Fotin I.A., Kayurov K.N., Buyakova S.P. Effect of heat treatment modes on structure and properties of 08Kh18N6AG10S steel. *Izvestiya. Ferrous Metallurgy*. 2024;67(2):195–204. https://doi.org/10.17073/0368-0797-2024-2-195-204

Гордиенко А.И., Абдульменова Е.В., Козлова Т.В., Гоморова Ю.Ф., Власов И.В., Фотин И.А., Каюров К.Н., Буякова С.П. Влияние режимов термической обработки на структуру и свойства стали 08Х18Н6АГ10С. *Известия вузов. Черная металлургия*. 2024;67(2):195–204. https://doi.org/10.17073/0368-0797-2024-2-195-204

22. Zuev L.B., Barannikova S.A., Maslova O.A. The features of localized plasticity autowaves in solids. *Materials Research*. 2019;22(4):104–123. http://doi.org/10.1590/1980-5373-mr-2018-0694

23. Zuev L.B., Barannikova S.A. Autowave physics of material plasticity. *Crystals*. 2019;9(9):458. https://doi.org/10.3390/cryst9090458

24. Zuev L.B., Khon Yu.A. Plastic flow as spatiotemporal structure formation. Part I. Qualitative and quantitative patterns. *Physical Mesomechanics*. 2022;25(2):103–110. https://doi.org/10.1134/S1029959922020011

25. Zuev L.B., Gorbatenko V.V., Pavlichev K.V. Elaboration of speckle photography techniques for plastic flow analyses. *Measurement Science and Technology*. 2010;21(5):054014. http://doi.org/10.1088/0957-0233/21/5/054014

26. Mendenhall W.M., Sincich T.L. Statistics for Engineering and the Sciences. New York: Chapman and Hall/CRC; 2016:1182.

Information about the Authors / Сведения об авторах

Svetlana P. Buyakova, *Dr. Sci. (Eng.), Chief Researcher, Head of the Laboratory of Physical Mesomechanics and Non-Destructive Testing,* Institute of Strength Physics and Materials Science, Siberian Branch of the Russian Academy of Sciences
ORCID: 0000-0002-6315-2541
E-mail: sbuyakova@ispms.ru

Konstantin N. Kayurov, *General Director,* LLK Scientific Production Enterprise of Geophysical Equipment "Luch"
ORCID: 0000-0001-9545-5400
E-mail: kayurov@looch.ru

Svetlana A. Barannikova, *Dr. Sci. (Phys.-Math.), Leading Researcher of the Laboratory of Strength Physics,* Institute of Strength Physics and Materials Science, Siberian Branch of the Russian Academy of Sciences
ORCID: 0000-0001-5010-9969
E-mail: bsa@ispms.ru

Светлана Петровна Буякова, *д.т.н., главный научный сотрудник, заведующий лабораторией физической мезомеханики и неразрушающих методов контроля,* Институт физики прочности и материаловедения Сибирского отделения РАН
ORCID: 0000-0002-6315-2541
E-mail: sbuyakova@ispms.ru

Константин Николаевич Каюров, *генеральный директор,* ООО Научно-производственное предприятие геофизической аппаратуры «ЛУЧ»
ORCID: 0000-0001-9545-5400
E-mail: kayurov@looch.ru

Светлана Александровна Баранникова, *д.ф.-м.н. ведущий научный сотрудник лаборатории физики прочности,* Институт физики прочности и материаловедения Сибирского отделения РАН
ORCID: 0000-0001-5010-9969
E-mail: bsa@ispms.ru

Contribution of the Authors / Вклад авторов

S. P. Buyakova – concept formulation, literary review, analysis of the results.
K. N. Kayurov – selection of laser surfacing modes, discussion of the results.
S. A. Barannikova – conducting studies on mechanical characteristics and heterogeneity of deformation, discussion of the results, writing the text.

С. П. Буякова – формулирование концепции работы, обзор литературы, анализ результатов.
К. Н. Каюров – подбор режимов лазерной наплавки, обсуждение результатов.
С. А. Баранникова – проведение исследований механических характеристик и неоднородности деформации, обсуждение результатов, написание текста статьи.

Received 03.06.2024
Revised 21.08.2024
Accepted 20.09.2024

Поступила в редакцию 03.06.2024
После доработки 21.08.2024
Принята к публикации 20.09.2024